Amino Acids (2014) 46:1681–1696
DOI 10.1007/s00726-014-1728-9

ORIGINAL ARTICLE

Radiation protection from whole-body gamma irradiation (6.7 Gy): behavioural effects and brain protein-level changes by an aminothiol compound GL2011 in the Wistar rat

Minu Karthika Ganesan · Milos Jovanovic · Bojana Secerov · Marija Ignjatovic · Martin Bilban · Andjus Pavle · Amal El Refaei · Gangsoo Jung · Lin Li · Ajinkya Sase · Weiqiang Chen · Goran Bacic · Gert Lubec

Received: 27 February 2014 / Accepted: 10 March 2014 / Published online: 29 March 2014

Abstract GL2011 is a naturally occurring thiol compound and a series of thiol compounds have been proposed as radioprotectors. Radioprotective efficacy of a triple intraperitoneal dose of GL2011 of 100 mg/kg body weight of Wistar rats, 30 min prior to and 3 and 6 h following irradiation (6.7 Gy) was evaluated. Four groups of animals were used, vehicle-treated non-irradiated (VN), GL2011-treated and irradiated (GI), GL2011-treated and non-irradiated (GN) and vehicle-treated and irradiated (VI) ($n = 30$ per group). The radioprotective efficacy of GL2011 was determined by measuring 28-day survival and intestinal crypt cell survival. Neuroprotection in terms of behaviour was evaluated using the behavioural observational battery, open field test and elevated plus maze paradigm. An RNA microarray was carried out in order to show differences at the RNA level between VI and VN groups. Brain protein changes were identified using a gel-based proteomics method and major brain receptor complex levels were determined by blue-native gels followed by immunoblotting. 28-Day survival rate in VI was 30 %, in GI survival was 93 %, survival of VN and GN was 100 %. Jejunal crypt cell survival was significantly enhanced in GI. Protein-level changes of peroxiredoxin-5, Mn-superoxide dismutase 2, voltage-dependent anion-selective channel protein 1, septin 5 and dopamine D2 receptor complex levels were paralleling radiation damage and protection. Taken together, the findings demonstrate that GL2011 improves survival rates and jejunal crypt survival, provides partial neuroprotection at the

Electronic supplementary material The online version of this article (doi:10.1007/s00726-014-1728-9) contains supplementary material, which is available to authorized users.

M. K. Ganesan · A. E. Refaei · G. Jung · L. Li · A. Sase · W. Chen · G. Lubec (✉)
Department of Pediatrics, Medical University of Vienna, Währinger Gürtel 18, 1090 Vienna, Austria
e-mail: gert.lubec@meduniwien.ac.at

A. E. Refaei
e-mail: amal.elsaidelrefaei@univie.ac.at

G. Jung
e-mail: gsjung0402@gmail.com

L. Li
e-mail: linli411@gmail.com

A. Sase
e-mail: ajinkyasase@gmail.com

W. Chen
e-mail: chenweiqiang@gmail.com

M. Jovanovic · A. Pavle
Faculty of Biology, University of Belgrade, Belgrade, Serbia
e-mail: jovanovic@bio.bg.ac.rs

A. Pavle
e-mail: pandjus@bio.bg.ac.rs

B. Secerov · M. Ignjatovic
Vinca Institute of Nuclear Sciences, Belgrade, Serbia
e-mail: bojana@vin.bg.ac.rs

M. Ignjatovic
e-mail: markic1803@gmail.com

M. Bilban
Department of Laboratory Medicine, Medical University of Vienna and Core Facility Genomics, Core Facilities, Medical University of Vienna, Währinger Gürtel 18, 1090 Vienna, Austria
e-mail: martin.bilban@meduniwien.ac.at

G. Bacic (✉)
Faculty of Physical Chemistry, University of Belgrade, Belgrade, Serbia
e-mail: ggbacic@ffh.bg.ac.rs

behavioural level and modulates proteins known to be involved in protection against oxidative stress-mediated cell damage.

Keywords Radiation protection · Amino thiol · Survival · Blue-native gel · Mass spectrometry · Microarray · Crypt assay · Behaviour

Introduction

As early as in 1953 radiation protection by sulfhydryl-containing amino acids has been proposed by an experimental study (Perroy and Buchet 1953), and indeed it has been shown that even endogenous thiols play a role in radiation protection (Vos 1992). About a decade ago, Gadsen and Edwards (1964) suggested the use of naturally occurring sulphur-containing amino acids for radiation protection. About two decades later Williams and Denekamp (1983) showed that aminothiol WR-2721 was modifying the radiation response of the mouse and since then several WR-aminothiols were reported to act as radioprotectants (Carnes and Grdina 1992; Littlefield and Hoffmann 1993; Laayoun et al. 1994; Capizzi 1996; Diamond et al. 1996; Devi et al. 1998; Belkacémi et al. 2001; Bhattacharya et al. 2001; Evans et al. 2002); the role of the classical aminothiol amifostine was reviewed by Wassermann and Brizel (Wasserman and Brizel 2001). There are other thiol compounds unrelated to amino thiols that act as radioprotectants and these include thiodiazoles (Prouillac et al. 2009), vitamins (Kumar et al. 2002a), 5-thio-glucose (Schuman et al. 1983), selenomethionine (Ware et al. 2011) and D-methionine (Vuyyuri et al. 2008; Cotrim et al. 2012). Although some compounds exhibited tolerable toxicity, the search for non-toxic radio protectors is continuing (Kumar et al. 2002b).

The aim of the present study was to test a naturally occurring sulphur-containing aminothiol, GL2011, in a rat model of whole-body gamma irradiation. Studies on radiation protection in terms of survival, behavioural tests including the open field, elevated plus maze, neurological functional observational battery (FOB) were carried out in order to show behavioural consequences of irradiation and protection of brain functions by the proposed radioprotector GL2011. The severity of intestinal injury was determined as it is considered to be a determinant of lethality after total body irradiation. Transcriptional differences were tested by a microarray technique and studies were performed at the proteome level to show qualitative and quantitative protein changes caused by irradiation or GL2011 treatment by a gel-based proteomics method. Subsequently, major brain receptor complexes were studied in hypothalamus of rat brain leading to the identification of mediators of radiation damage at the protein level and the differentially expressed proteins were validated by immunoblotting.

Materials and methods

Animals

The experiments were performed using male albino Wistar rats weighing approximately 200 g (±5 %). Animals were reared and bred in Vinca Institute of Nuclear Sciences, Belgrade, and housed prior to and after irradiation at ambient temperature (20–23 °C) in cages (two animals per cage) 12/12 light/dark rhythm. Food and water were provided ad libitum.

Irradiation

A 60-cobalt gamma ray source designed for radiobiological and radiation chemistry experiments (Vinca Institute of Nuclear Sciences, Belgrade) was used for irradiation. Calibration of the source for these experiments was performed by measuring midline absorbed doses in agarose gel phantoms of a rat with embedded plastic vials (in the middle and at both sides of the phantom) containing Fricke solution and doses were determined by spectrophotometry. Based on literature data, the dose of 6.7 Gy was selected as a potential $LD_{50/30}$ dose (Logie et al. 1960). Non-anaesthetized animals were confined in custom-made individual cages made of wire, which were arranged in a circle around the source (6 rats per session) at around 25 cm from the source that was comparable to a previous publication (Logie et al. 1960) using similar setup and source. Total body irradiation was performed with rats sideways to the source at the dose rate of 0.41 Gy/min, i.e. 16 min of irradiation for the dose of 6.7 Gy. Since irradiation of rat phantoms indicated slight left–right dose gradient due to the proximity of animals to the source, cages with rats were sideways rotated by 180° at the middle of irradiation session to provide uniform dose distribution.

Experimental design

Rats in group I (GI) were irradiated with intraperitoneal GL2011-treatment at 30 min prior to irradiation as well as 3 and 6 h post-irradiation. Doses were 100 mg/kg body weight, administered in 1 mL vehicle (phosphate-buffered saline, PBS, pH 7.35). Rats in group II (VI) were treated with vehicle (PBS) at identical time points as the GI group and irradiated. Rats in group III (GN) were given i.p. injections of GL2011 in PBS (the same dose as in group I), but were not irradiated. Rats in group IV (VN) served as the sham-treated group, only vehicle was administered and

they were not irradiated. Following irradiation, animals were inspected twice a day (morning and evening) and moribund animals were killed according to the IACUC Guidelines, IACUC Policy#5. Experiments were done under licence and approvement from the Ministry of Agriculture, Forestry and Water Management, which includes an ethical evaluation of the project (Approval number 04/2012, 27.05.2012). Housing and maintenance of animals were in compliance with European and national regulations. Animals were killed by decapitation on a guillotine on day 29 from the onset of irradiation and organs were taken. Brains were taken for biochemical analyses and stored at −80 °C.

Survival analysis

Survival of rats from all the four groups was monitored from the day of onset of the experiment until the 28th day. The probabilities of the survival of all four groups were plotted as Kaplan–Meier survival curves until the 28th day. Significant differences in the survival curves among the groups VN, VI, GN and GI were evaluated using log rank test (Mantel–Cox test) for multiple groups.

Jejunal crypt cell survival assay

Following the killing, rat intestines were fixed in 10 % buffered formalin for 24–48 h at room temperature. The specimens were subsequently dehydrated in ascending alcohol concentrations, cleared with organic solvents, and subsequently embedded in paraffin. Paraffin blocks were cut into 5-μm-thick sections and stained with hematoxylin–eosin. Ten transverse sections of small intestine from each rat, taken at intervals of 80 μm, were used to estimate the number of villi and crypts. The number of intestinal villi and crypts was determined by using a computer-supported imaging analysis Pro 3.1 software system connected to a light microscope (Olympus AX70) with the objective magnification of 4× and 10× (Mitrović et al. 2012).

The number of regenerating crypts and the total number of crypts per transverse circumference were counted for ten histological jejunal cross-sections per rat. Determining the number of villi at the sections of the small intestine, villi were classified as normal (full-length villi reaching the gut lumen), as well as medium and small villi in length (not reaching the gut lumen). The total number of crypts per cross section was determined along with the number of full-length crypts with lumen, and small and medium-length crypts. Data obtained from each rat were averaged per intestinal section and standard deviation of the mean values was calculated. Statistical analysis was performed using one-way analysis of variance (ANOVA) with post hoc Bonferroni test for comparison between groups. The results are expressed as mean value ± standard deviations (SD) per section. Differences at $p < 0.05$ were accepted as the level of significance (Mitrović et al. 2012).

Behavioural studies

The Elevated plus maze study and the Open field test were performed between 12th and 14th day from the onset of the experiment.

Open field (OF)

Rats were observed with a video monitoring system (video camcorder: 1/3 in. SSAM H EX VIEW HAD coupled to the computerized tracking system: TiBeSplit) in an arena (100 cm × 100 cm long; with 40-cm-high walls) for 10 min. Rats were placed into the centre of the arena and following parameters were measured: path length, resting time, percentage of local and large movements, average speed, number of times crossing centre, frequency of spontaneous changes and time spent on the periphery (Prut and Belzung 2003).

Elevated plus maze (EPM)

The maze consisted of 4 arms (each 50 cm long and 10 cm wide) fixed to the height of 50 cm, and the arms were interconnected by a 10 cm × 10 cm wide central area. Two arms had 30-cm-high side and end walls. Rats were observed for 5 min with a video camcorder coupled to a computerized tracking system in an arena. Rats were placed in the central area, head pointing away from the box. Rats were observed for anxiety-related behaviour. The parameters recorded were time spent in open and closed arm, number of entries into the open and closed arm, and path length in open and closed arm. An entry was defined as having the animal place all four legs into the box (Pellow et al. 1985).

Neurological functional observational battery

Various neurological functions were checked as listed in Supplementary Table 1. The FOB screening was based on Irwin (1968) and SHIRPA (Rogers et al. 2001) protocols. A battery of tests was applied to determine changes in spontaneous activity, motor-affective responses, sensory motor response, posture, muscle tone, gait and excretion. To complete the assessment, vitally important reflexes like pinna reflex, toe pinch, touch escape, etc., were scored.

Microarray analysis

Total RNA was isolated from hypothalamus of rats (6 per group) from VI and VN groups using the RNeasy® micro

kit (© 2003–2007 QIAGEN). Total RNA (200 ng) was then used for GeneChip analysis. Preparation of terminal-labeed cDNA, hybridization to genome-wide Rat Gene Level 1.0 ST GeneChips (Affymetrix) and scanning of the arrays were carried out according to manufacturer's protocols (https://www.affymetrix.com). Robust multi-array average (RMA) signal extraction, normalization and filtering were performed using a custom chip description file (Dai et al. 2005). A standard variation filter was applied for selecting informative (i.e. significantly varying) genes using CARMAweb (Rainer et al. 2006) statistical group comparisons. To calculate differential gene expression between individual sample groups, we performed a statistical comparison using the LIMMA package as described previously (Astapova et al. 2008). Briefly, LIMMA estimates the fold change between predefined sample groups by fitting a linear model and using an empirical Bayes method to moderate the standard errors of the estimated log-fold changes for each probe set. A multiple testing correction based on the false discovery rate (FDR) was performed to produce adjusted *p* values (Smyth 2005).

Validation of microarray studies at the protein level

Immunoblotting

Protein concentrations of brain lysates were measured using the bicinchoninic acid assay using Pierce™ BCA Protein Assay (Smith et al. 1985). The lysates, 10 replicates from VN, VI, GN and GI each containing 30 µg of total protein were run on 10 % SDS gels (Criterion cell 1D electrophoresis system, Bio-Rad Laboratories) before being transferred to a PVDF membrane (Millipore-45 µm pore size) in transfer buffer (48 mM Tris, 39 mM glycine, 0.03 % SDS) at 23 °C using a semi-dry Bio-Rad transfer system. The membrane was blocked with 5 % (w/v) milk powder in 1× TBST (100 Mm Tris–HCL, 150 mM NaCl, 0.1 % Tween 20, pH 7.5) at 23 °C for at least 1 h before probing the protein bands with antibodies against Aadat (Anti-aminoadipate aminotransferase antibody, ab89608-abcam) and RT1 AW2 (Anti-RT1-Aw2 antibody, ab119782-abcam). The blocked membranes were then probed with the Aadat antibody (1:2,000) or RT1 AW2 antibody (1:4,000) in 1 % BSA in 1× TBST and incubated at 4 °C overnight. After washing the membranes six times using 1× TBS with 0.1 % Tween 20, they were incubated with horseradish peroxidase-conjugated rabbit polyclonal secondary antibody to mouse IgG (ab97046-abcam) (1:10,000) in 5 % (w/v) milk powder in 1× TBST at 23 °C for 1 h followed by further washing using 1× TBST. Membranes were developed with the Amersham ECL plus Western blotting detection system (GE Healthcare). The Coomassie staining of total proteins on the PVDF membrane after transfer using 0.1 % Coomassie R-350 in methanol/distilled water was used as loading control as described in Welinder and Ekblad (2011). The developed films were scanned using Bio-Rad Chemidoc™ MP system. Protein bands were quantified by densitometry using Bio-Rad Image Lab™ software. Statistics was performed by Graph Pad Prism 6 (Graph Pad Software, Inc. CA, USA). Results were calculated as mean ± SD. Statistical significance was determined using two-way ANOVA and Tukey Kramer post hoc tests to analyse differences between the four groups. Statistical significance was considered at the stringent conditions of $***p < 0.001$.

2D electrophoresis

Sample preparation

Cerebellum from each rat from all the four groups (eight per group) were homogenized and suspended in 1.8 mL sample buffer (20 mM Tris, 7 M urea, 2 M thio urea, 4 % w/v CHAPS, 10 mM 1,4-dithioerythritol, 1 mM EDTA, 1 mM PMSF, 1 tablet Complete™ (Roche Diagnostics, Switzerland) and 0.2 % v/v phosphatase inhibitor cocktail from Calbiochem, Merck, Darmstadt, Germany). The suspension was sonicated on ice for approximately 30 s and centrifuged at 14,000×*g* for 60 min at 12 °C. Desalting was carried out with an Ultrafree-4 centrifugal filter unit at a cut-off molecular weight of 10,000 Da (Millipore, Bedford, MA, USA) at 4,400×*g* at 12 °C until the eluted volume was about 4 mL and the remaining volume reached 100–200 µL. The protein content of the supernatant was determined by the Bradford assay (Bae et al. 2012).

Two-dimensional gel electrophoresis (2-DE)

2-DE was performed essentially as reported previously (Bae et al. 2012). Samples containing 700 µg of protein (8 gels per group) were subjected to immobilized pH 3–10 nonlinear gradient strips. Focusing started at 200 V. The voltage was gradually increased to 8,000 V at 4 V/min and kept constant for further 3 H (approximately 150,000 Vh totally). Prior to the second-dimensional run, strips were equilibrated twice for 15 min with gentle shaking in 10 mL of SDS equilibration buffer (50 mM pH 8.8 Tris–HCl, 6 M urea, 30 % v/v glycerol, 2 % w/v SDS, trace of bromophenol blue). DTT (1 %) w/v was added at the first incubation for 15 min and 4 % iodoacetamide w/v instead of DTT at the second incubation step for 15 min. The second-dimensional separation was performed on 10–16 % gradient SDS-PAGE. After protein fixation for 12 h in 50 % methanol and 10 % acetic acid, the gels were stained with colloidal Coomassie blue (Novex, San Diego, CA, USA) for 8 h and excess of dye was washed out from the gels

with distilled water. Molecular masses were determined by running precision protein standard markers (Bio-Rad Laboratories, Hercules, CA, USA), covering the range of 10–250 kDa. Isoelectric point values were determined as given by the supplier (GE Healthcare, Buckinghamshire, UK) of the immobilized pH gradient strips.

Quantification of protein levels

Protein spots from each gel were outlined (first automatically and then manually) and quantified using the PDQuest 2-D analysis software version 8.0 (© 2005 Bio-Rad Laboratories). The percentage of the volume of the spots representing a certain protein was determined in comparison with the total proteins present in the 2-DE gel. The software used also revealed that spots evaluated did not contain other proteins. Moreover, only well-separated spots were considered for quantification. A total of 525 distinct protein spots were identified by the software which was then re-evaluated manually. Two-way ANOVA was performed comparing the volume of all 525 spots among the already mentioned 4 groups ($***p < 0.001$, two-way ANOVA, post hoc Tukey test). Among the spots quantified, seven spots were significantly different among the four groups. These spots were chosen for identification using Nano-LC-ESI-(CID/ETD)–MS/MS (high-capacity ion trap, HCT).

Analysis of peptides by nano-LC-ESI-(CID/ETD)–MS/MS (high-capacity ion trap)

The spots that showed significant differences were manually excised and placed into 1.5-mL LoBind Eppendorf tubes. Gel plugs were washed with 10 mM ammonium bicarbonate and 50 % ACN in 10 mM ammonium bicarbonate repeatedly. The addition of 100 % ACN resulted in gel shrinking and the shrunk gel plugs were then dried in a Speedvac Concentrator, 5301 (Eppendorf, Germany). The dried gel pieces were reswollen and in-gel digested with 40 ng/mL trypsin (Promega, Madison, WI, USA) in digestion buffer, consisting of 5 mM octyl β-D-glucopyranoside (OGP) and 10 mM ammonium bicarbonate, and incubated over night at 37 °C. Peptide extraction was performed with 10 mL of 10 mM ammonium bicarbonate overnight, 15 mL of 1 % formic acid (FA) in 5 mM OGP for 30 min, 15 mL of 0.1 % FA for 30 min, and subsequently 0.1 % FA in 20 % ACN for 30 min. The extracted peptides were pooled for high-capacity ion trap (HCT) analysis. In total, 40 µL of extracted peptides was analysed by HCT. The HPLC used was a bio-compatible Ultimate 3000 system (Dionex, Sunnyvale, CA, USA) equipped with a PepMap100 C-18 trap column (300 mm × 5 mm) and PepMap100 C-18 analytic column (75–150 mm). The gradient was (A: 0.1 % FA in water, B: 0.08 % FA in ACN) 4–30 % B from 0 to 105 min, 80 % B from 105 to 110 min, 4 % B from 110 to 125 min. The flow rate was 300 nL/min from 0 to 12 min, 75 nL/min from 12 to 105 min, and 300 nL/min from 105 to 125 min. A HCT ultra-PTM discovery system (Bruker Daltonics, Bremen, Germany) was used to record peptide spectra over the mass range of *m/z* 350–1,500, and MS/MS spectra in information-dependent data acquisition over the mass range of *m/z* 100–2,800. Repeatedly, MS spectra were recorded followed by three data-dependent CID MS/MS spectra and three ETD MS/MS spectra generated from three highest intensity precursor ions. An active exclusion of 0.4 min after two spectra was used to detect low abundant peptides. The voltage between ion spray tip and spray shield was set to 1,100 V. Drying nitrogen gas was heated to 170 °C and the flow rate was 10 L/min. The collision energy was set automatically according to the mass and charge state of the peptides chosen for fragmentation. Multiple-charged peptides were chosen for MS/MS experiments based on their good fragmentation characteristics. MS/MS spectra were interpreted and peak lists were generated by DataAnalysis 4.0 (Bruker Daltonics, Bremen Germany). Searches were done by using MASCOT 2.2.04 (Matrix Science London, UK) against the latest UniProtKB (http://www.uniprot.org) for protein identification. Searching parameters were set as follows: enzyme selected as trypsin with maximum of two missing cleavage sites, species limited to "Rat", a mass tolerance of 0.2 Da for peptide tolerance, 0.2 Da for MS/MS tolerance, fixed modification of carbamidomethyl (C), and variable modification of methionine oxidation and phosphorylation (Tyr, Th, and Ser). Positive protein identifications were based on a significant MOWSE score. After protein identification, an error-tolerant search was done to detect nonspecific cleavage and unassigned modifications. Protein identification and modification information returned from MASCOT were manually inspected and filtered to obtain confirmed protein identification and modification lists of CID MS/MS and ETD MS/MS (Bae et al. 2012).

Western blotting

Thirty microgram of rat cerebellar protein extracts from all four experimental groups was loaded onto 1D SDS-PAGE gels. Proteins were transferred at 23 °C onto PVDF membranes (Millipore, 45 µm pore size) using a semi-dry Bio-Rad transfer system. Membranes were blocked by incubation for 1 H in TBST containing 5 % non-fat dried milk powder (Bio-Rad) and 0.1 % Tween 20. After washing, membranes were incubated with diluted primary antibodies: anti-SEPT5 antibody-ab69538 (1:2,500; Abcam, Cambridge, UK), anti-peroxiredoxin 5 antibody (1:2,000; Abcam, Cambridge, UK), anti-VDAC 1 antibody

(1:1,000; Abcam, Cambridge, UK) and anti-SOD2 antibody (1:5,000; Abcam, Cambridge, UK) at 4 °C overnight. Membranes were washed three times by gentle agitation in TBST containing 0.1 % Tween 20. The anti-SOD2 antibody and anti-VDAC 1 antibody were detected with HP-coupled secondary anti-rabbit IgG (1:5,000; Abcam, Cambridge, UK). The anti-SEPT5 antibody and anti-peroxiredoxin 5 primary antibodies were detected with rabbit polyclonal secondary antibody to mouse IgG—H&L (1:5,000; ab97046; Abcam, Cambridge, UK). Membranes were developed with the Amersham ECL plus Western blotting detection system (GE Healthcare, Buckinghamshire, USA).

Determination of brain receptor complexes by blue-native gels and subsequent immunoblotting

Ten hypothalami from each of the four groups were run on blue-native PAGE followed by immunoblotting with antibodies against major brain receptor systems 5-hydroxytryptamine 1A (5HT1A, serotonin receptor 1A, 1:25,000), AMPA receptors (GluR1-1:20,000 and GluR2-1:10,000), NMDA receptor (NR1, 1:5,000) dopamine receptors (D1-1:5,000 and D2-1:10,000) and nicotinic acetylcholine receptors alpha 4 and alpha 7 (Nic4-1:10,000, Nic7-1:5,000) as given below.

Sample preparation

Samples were homogenized in ice-cold homogenization buffer [10 mM, HEPES, pH 7.5, 300 mM sucrose, one complete protease inhibitor tablet (Roche Molecular Biochemicals, Mannheim, Germany) per 50 mL by Ultra-Turrax (IKA, Staufen, Germany). The homogenates were centrifuged for 10 min at 1,000×*g* and the pellet was discarded. The supernatant was centrifuged at 50,000×*g* for 30 min in an ultracentrifuge (Beckman Coulter Optima_L-90K). Subsequently, the pellet was homogenized in 5 mL washing buffer (homogenization buffer without sucrose), kept on ice for 30 min and centrifuged at 50,000×*g* for 30 min.

Sucrose gradient ultracentrifugation for membrane fractionation

The plasma membrane purification procedures from the pellet were carried out as described previously, with slight modification. Sucrose density gradient centrifugation solutions of 700 µL each of 69, 54, 45, 41, and 37 % (w/v) were formed. Membrane pellets in 500 µL were re suspended in homogenization buffer, layered on top of the tubes that were filled with homogenization buffer. Samples were ultracentrifuged at 4 °C at 70,000×*g* for 3 h. After centrifugation, the 41 % fraction from the sucrose interface was collected, diluted 10 times with homogenization buffer, and then ultracentrifuged at 4 °C at 100,000×*g* for 30 min. After discarding the supernatant, the pellet was stored at −80 °C until use (Chen et al. 2006; Ghafari et al. 2011).

Blue native-polyacrylamide gel electrophoresis (BN-PAGE)

Membrane pellets from the 41 % sucrose gradient ultracentrifugation fraction were solubilized in extraction buffer (1.5 M 6-aminocaproic acid, 300 mM Bis–Tris, pH 7.0) and 10 % Triton X-100 (stock solution was added at a ratio of 1:4 to achieve final 2 % Triton X-100 concentration) with vortexing every 10 min for 1 h. Following solubilization, samples were cleared by centrifugation at 20,000×*g* for 60 min at 4 °C. The protein content was estimated using the BCA protein assay kit (Pierce, Rockford, IL, USA). Fifty microgram of the membrane protein preparation was applied onto gels. Sixteen millilitres BN-PAGE loading buffer [5 % (w/v) Coomassie G250 in 750 mM 6-aminocaproic acid] were mixed with 100 µL of the membrane protein preparation and loaded onto the gel. BN-PAGE was performed in a PROTEAN II xi Cell (Bio-Rad, Germany) using 4 % stacking and 5–18 % separating gel. The BN-PAGE gel buffer contained 500 mM 6-aminocaproic acid, 50 mM Bis–Tris, pH 7.0; the cathode buffer 50 mM Tricine, 15 mM Bis–Tris, 0.05 % (w/v) Coomassie G250, pH 7.0; and the anode buffer 50 mM Bis–Tris, pH 7.0. The voltage was set to 50 V for 1 h, 75 V for 6 h, and was increased sequentially to 400 V (maximum current 15 mA/gel, maximum voltage 500 V) until the dye front reached the bottom of the gel (Kang et al. 2008). Native high molecular mass markers were obtained from Invitrogen (Carlsbad, CA, USA).

Immunoblotting

Membrane proteins were transferred from BN-PAGE to PVDF membranes. After blocking of membranes for 1 h with 10 % non-fat dry milk in 0.1 % TBST (100 mM Tris–HCL, 150 mM NaCl, pH 7.5, 0.1 % Tween 20), membranes were incubated with primary antibodies GluR1 (Abcam, ab31232, Cambridge, UK), GluR2 (Abcam, ab52932, Cambridge, UK), GluR3 (Abcam, ab87609, Cambridge, UK), GluR4 (Abcam, ab109431, Cambridge, UK), Dopamine receptor D1 (Abcam, ab85608, Cambridge, UK), Dopamine Receptor D2 (Millipore, AB5084P), nicotinic Acetylcholine Receptor alpha4 (Abcam, ab41172, Cambridge, UK), nicotinic Acetylcholine Receptor alpha7 (Abcam, ab10096, Cambridge, UK), Muscarinic Receptor M1 (Abcam, ab75178, Cambridge, UK), NMDAR1 (Abcam, ab28669, Cambridge, UK), $5HT1_A$ (GenScript, Piscataway, NJ, USA), and detected with horseradish peroxidase-conjugated anti-rabbit IgG (Abcam, ab6721, Cambridge, UK). Membranes were developed with the ECL Plus Western Blotting Detection System (GE Healthcare, Buckinghamshire, UK). Arbitrary optical densities of immunoreactive bands were measured by the Image J software program.

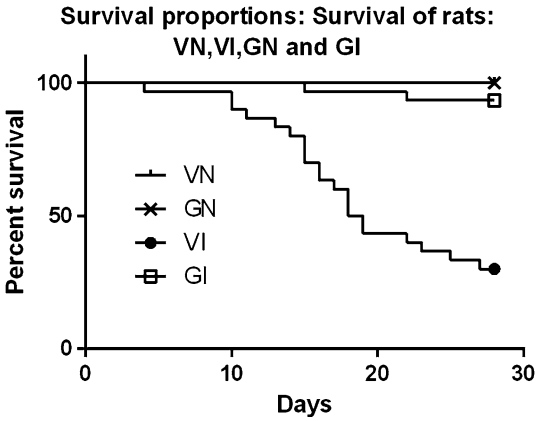

Fig. 1 Kaplan–Meier survival analysis. Comparison of survival percent of rats among the four groups VN, VI, GI and GN, using Kaplan–Meier survival analysis. The survival curves were significantly different as predicted by log rank test. (***p value <0.001)

Results

Survival analysis

Figure 1 demonstrates radioprotective capability of GL2011 leading to a survival of 93 % of rats in the GI group as compared to a survival of 30 % in the VI group. The survival in non-irradiated groups GN and VN was 100 %. The log rank test performed indicated that the survival curves were significantly different.

Crypt assay

Figure 2a, c shows that the small intestine of animals from the GN group closely resembles the structure with normal villi (the VN group) except for slightly more apparent presence of atypical ramified villi which can be the results

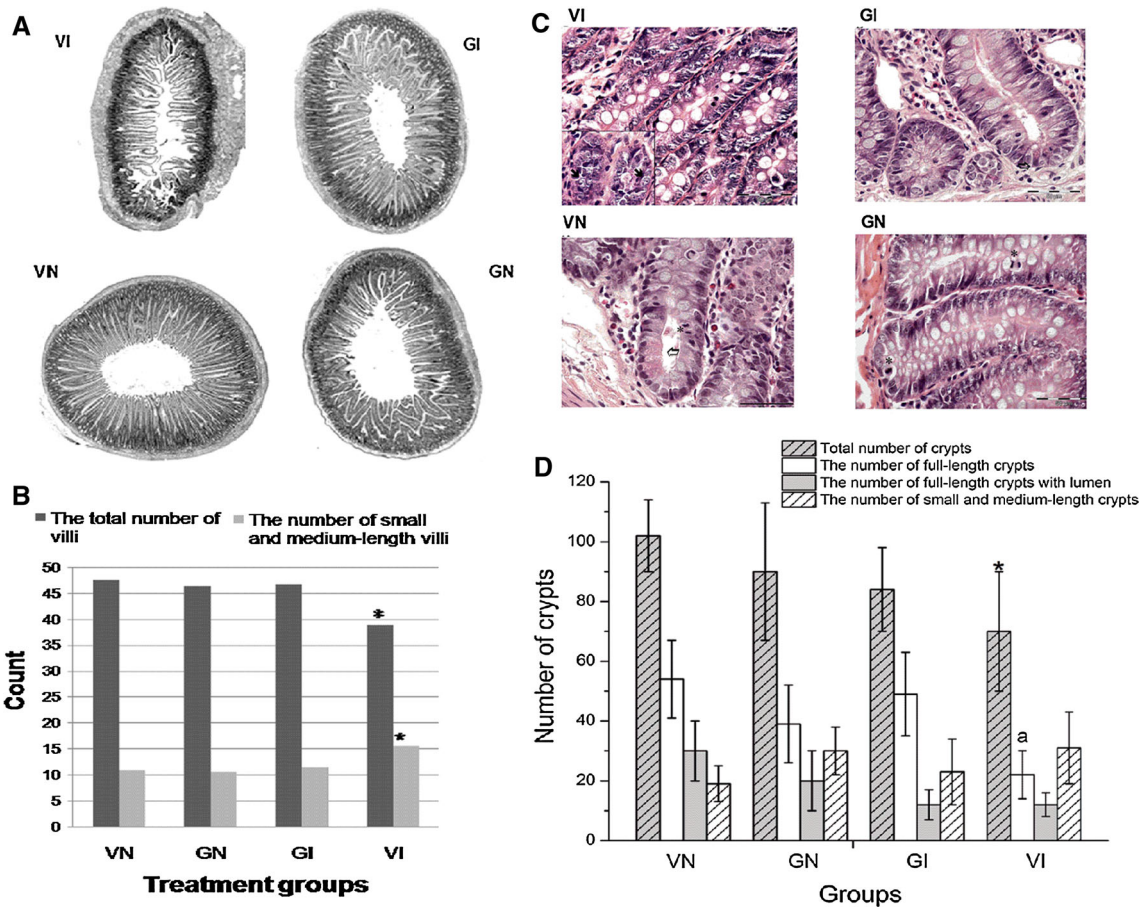

Fig. 2 Jejunal crypt cell assay. **a** Examples of micrographs of jejunal morphology (*VI* vehicle-treated and irradiated, *VN* vehicle-treated and non-irradiated, *GN* GL2011 treated and non-irradiated, and *GI* GL2011 treated and irradiated). The destruction of villi is apparent in the VI group. **b** Effect of GL2011 on the number of villi in four groups.The total number of villi is decreased and the number of small and medium length is increased in the VI group as compared to the other three groups (*$p < 0.05$). **c** Examples of micrographs of jejunal morphology with crypts for four different treatments. Viable cells are present in crypts of VN, GN, and GI groups, while they are scarce in the VI group (*insert*, *the closed arrow*). Paneth cells (*the open arrow*) and cells undergoing division (*) can be appreciated. *Horizontal bar* indicates 50 μm. **d** Effect of GL2011 on jejunal crypt cell survival. Counts of total crypts, full-length crypts with lumen and small and medium-length crypts. *$p < 0.05$ (as compared to VN), *a* $p < 0.05$ (as compared to VN and GI)

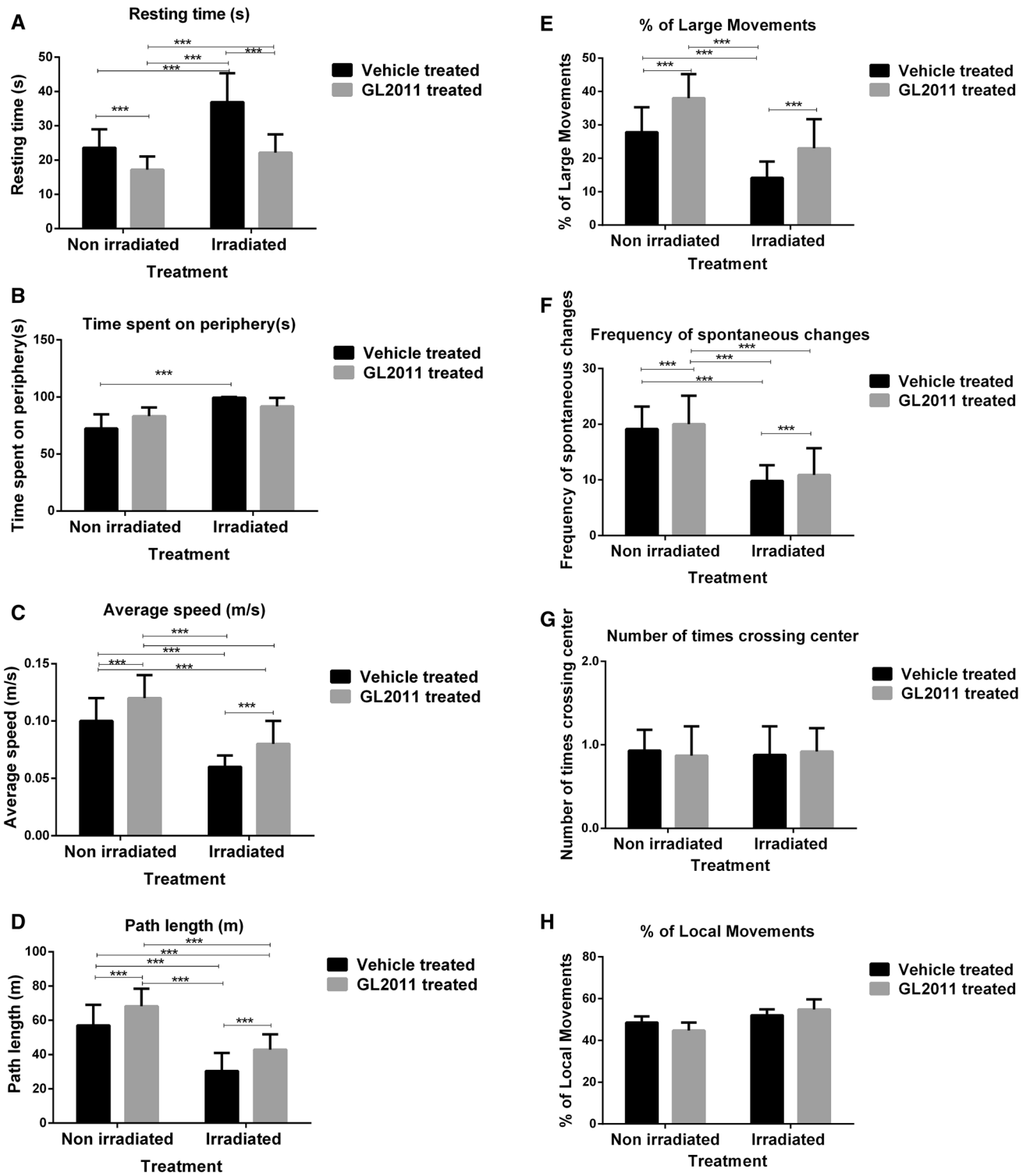
A
Resting time (s)
Resting time (s)
Vehicle treated
GL2011 treated
Non irradiated
Irradiated
Treatment
B
Time spent on periphery(s)
Time spent on periphery(s)
Vehicle treated
GL2011 treated
Non irradiated
Irradiated
Treatment
C
Average speed (m/s)
Average speed (m/s)
Vehicle treated
GL2011 treated
Non irradiated
Irradiated
Treatment
D
Path length (m)
Path length (m)
Vehicle treated
GL2011 treated
Non irradiated
Irradiated
Treatment
E
% of Large Movements
% of Large Movements
Vehicle treated
GL2011 treated
Non irradiated
Irradiated
Treatment
F
Frequency of spontaneous changes
Frequency of spontaneous changes
Vehicle treated
GL2011 treated
Non irradiated
Irradiated
Treatment
G
Number of times crossing center
Number of times crossing center
Vehicle treated
GL2011 treated
Non irradiated
Irradiated
Treatment
H
% of Local Movements
% of Local Movements
Vehicle treated
GL2011 treated
Non irradiated
Irradiated
Treatment

◀**Fig. 3** Results of open field test **a** and **b**. The resting time (**a**) and the time spent in the periphery (**b**) increased significantly in the VI rats when compared to the VN rats. GL2011 treatment (the GI group) significantly reversed the effect of radiation on resting time, but did not have effect on the time spent on periphery. A decrease in the resting time was observed following the administration of GL2011 in the GN group when compared to the VN group, but the time spent on periphery was not altered. The statistical analysis used was two-way ANOVA with Tukey post hoc test, $***p < 0.001$. **c–f** Average speed, path length, percentage of large movements and frequency of spontaneous changes decreased significantly in VI rats when compared to VN rats. GL2011 treatment significantly reversed the effect of radiation on average speed (**c**), path length (**d**), percentage of large movements (**e**) and frequency of spontaneous changes (**f**). Drug effects were seen as GL2011 increased average speed, path length and percentage of large movements in GN rats when compared to VN rats. The statistical analysis used was two-way ANOVA with Tukey post hoc test, $***p < 0.001$. **g**, **h** Radiation and/or GL2011-treatment did not change the parameters number of times crossing the centre (**g**) and % of local movements (**h**)

of normal villi regeneration. The number of total and small- and medium-length villi was essentially the same between these groups indicating that administration of GL2011 had no effect on the population of villi (Fig. 2b). The most apparent observation in the GI group is that it shows no significant difference from the VN and the GN groups in both categories of villi. However, the total number of villi was significantly reduced in the VI group as compared to the other groups (Fig. 2b). This is caused by the decrease of the population of normal length villi. In some parts there are only medium and small villi and consequently, the number of these structures was significantly increased in this group when compared to the other three groups, probably a sign of regeneration of villi. Nevertheless, the total crypt counts were significantly reduced in the VI group as compared to the other three treatments (Fig. 2d). Also, the number of full-length crypts in the VI group was significantly lower than in the protected GI group. All these findings unambiguously demonstrate a radioprotective effect of GL2011 in the GI group. No significant effect of GL2011 itself on crypts was observed.

Behavioural studies

Open field test

Resting time and time spent in the periphery increased significantly in the VI group when compared to VN group (Fig. 3a, b). Radiation reduced average speed (Fig. 3c), path length (Fig. 3d), percentage of large movements (Fig. 3e) and frequency of spontaneous changes (Fig. 3f). GL2011 significantly reversed the effect of radiation on all the above parameters (Fig. 3a–f) except for the time spent in the periphery (Fig. 3b). However, GL2011-treatment did not change the number of times crossing the centre (Fig. 3g) and % of local movements (Fig. 3h).

Drug effects, non-related to irradiation were also observed as GL2011 increased average speed, path length and percentage of large movements and decreased the resting time in animals from the GN group, compared to the VN group.

Elevated plus maze

The significant increase in the resting time was observed in the VI group as compared to the VN group (Fig. 4a). On the other hand, Fig. 4b, c shows that the pathlength in the open arms (left and right) as well as the time spent in the open arm (Fig. 4d) were significantly reduced in VI when compared to VN. Pre-treatment with GL2011 did not reverse the effects of irradiation on the resting time (Fig. 4a), but it reversed the effects of irradiation on the pathlength in the open arm and the time spent in the open arm. The drug effects of GL2011 are shown as increased path length in the open arms, the time spent in the open arm and decreased resting time in the GN group as compared to the VN group.

Neurological functional observational battery

All rats completed behavioural testing and results of the Neurological Functional Observational Battery are shown in Supplementary table 1. Scores (mean ± SD) are evaluated according to Irwin et al. Higher score presented more (better, higher) activity (performance, response) for all parameters except gait, wire manoeuvre and righting reflex whereas better performance was presented by a lower score. Some parameters are scored as ±positive/negative (two-way ANOVA, $*p < 0.05$, $**p < 0.01$, $***p \leq 0.001$). Major findings were tremors observed in the rats from group VI, while it was absent in VN, GN and GI groups. The parameters defining spontaneous activity, motor-affective response and muscle tone showed significant difference among the four groups, with the score being less in VI group indicating poor performance compared to VN group. GI group presented with improved performance when compared to VI group as evidenced by increased score.

Neurochemical findings

RNA microarray

Differences between RNA levels from hypothalami of VI and VN groups were considered significant when a twofold difference was observed in mean fold change and only four RNAs showed such difference based on the stringent

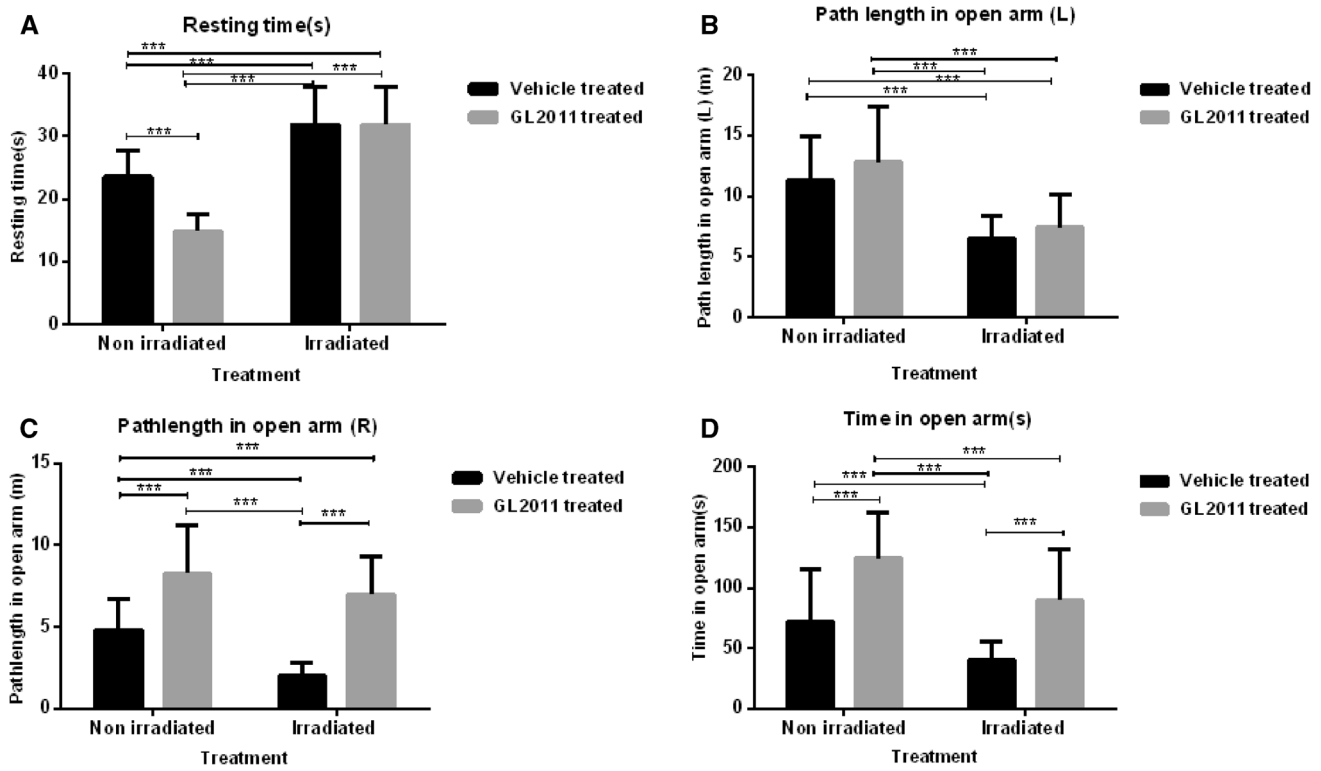

Fig. 4 Results of elevated plus maze. **a** The resting time increased significantly in VI rats when compared to VN rats. GL2011 treatment did not reverse the effects in terms of resting time in GI rats. Drug effects were seen as GL2011 decreased the resting time in GN rats when compared to VN rats. The statistical analysis used was two-way ANOVA with Tukey post hoc test, $***p < 0.001$. **b–d** Pathlength in the open arms (*left and right*) as well as time spent in the open arm was significantly reduced in VI rats when compared to VN rats. GL2011 treatment significantly reversed the effects of radiation in terms of pathlength in the open arm and the time spent in the open arm. The drug effects by GL2011 increased the pathlength in the open arm (R) and the time spent in the open arm in GN rats when compared to VN rats. The statistical analysis used was two-way ANOVA with Tukey post hoc test, $***p < 0.001$

criterion. Data on the outcome are listed in Table 1, showing that RNAs aminoadipate aminotransferase (Aadat) and RT1 AW2 were different in mean fold change at least twofold along with NA and MGC108823.

Validation of microarray studies at the protein level

Western blot performed to confirm the microarray data (Fig. 5a, b), where the expression of Aadat and RT1 AW2 genes showed more than twofold increase in the VI rats when compared to the VN rats, reflected the microarray results in cases of both Aadat and RT1 AW2 proteins. The two-way ANOVA results showed that increase in levels of Aadat protein and RT1 AW2 protein in VI rats when compared to VN was significant ($***p < 0.001$, two-way ANOVA, post hoc Tukey test). The levels of RT1 AW2 protein and Aadat protein were decreased significantly in the GI group when compared to VI group. GL2011 also significantly increased the levels of both proteins when administered without irradiation (in GN group) as compared to the VN group.

Two-dimensional gel electrophoresis

Proteins from cerebella of four experimental groups of rats (VN, VI, GN, and GI) were extracted and separated on 2DE gels. Protein spots showing significant differences in their spot intensity (Fig. 6) among the four groups were identified by mass spectrometry, and were labelled by their UniProtKB accession numbers. Identification results are provided in Table 2. The proteins that showed significant differences among all the four groups following the two-way ANOVA were unambiguously identified. Five proteins: vimentin-VIME_RAT (Spot 1708), septin 5-SEPT5_RAT (Spot 5512), voltage-dependent anion-selective channel protein 1-VDAC1_RAT (spot 8204), superoxide dismutase 2 (Mn)—SODM_RAT (Spot 7210) and mitochondrial peroxiredoxin-5-PRDX5_RAT (Spot 6105) were significantly increased in the VI group as compared to the VN group. GL2011 significantly increased their levels in the GI group when compared to the VI group. The drug effect of the GL2011 was observed by the significant increase of levels of these proteins in the GN group as compared to the VN group.

Table 1 Microarray gene chip data of significantly differentially expressed RNAs between VN and VI groups

Probe set_id	Accession number	Gene symbol	Corrected *p* value	Mean fold change (irradiated/not irradiated)
ENSRNOG00000030339_at	NA	NA	0.000198694	2.90
ENSRNOG00000019542_at	NM_001012353	MGC108823;RGD1559715	0.006251925	2.28
ENSRNOG00000011861_at	NM_017193;NP_058889	Aadat	0.000098618	2.22
ENSRNOG00000038999_at	NM_012645	RT1-EC2;RT1-A1;RT1-AW2	0.014733044	2.17

RNA levels from hypothalami showing four RNAs with the mean fold change VI/VN higher than two. Also shown are the gene symbols, probe set id, mean fold change and corrected p value

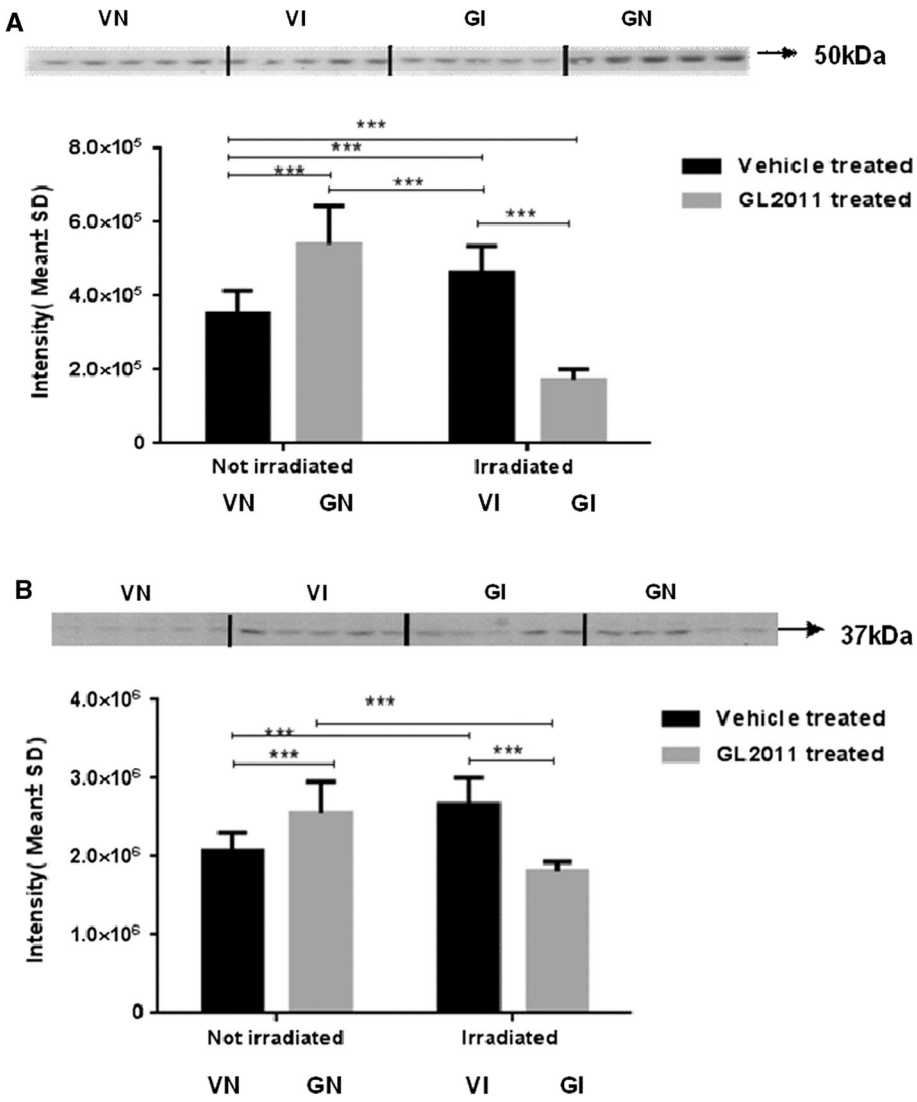

Fig. 5 Validation of microarray studies at the protein level **a**. Representative immunoblot image of aminoadipate aminotransferase comparing VN, VI, GI and GN groups. A target band for Aadat protein was observed at the expected apparent molecular weight (47.8 kDa). The total protein Coomassie R-350 staining of the PVDF membrane was used as the loading control. Densitometry analysis was performed to quantify the levels of Aadat in all four groups.The *graph* is representing the results of two-way ANOVA and Tukey post hoc confirmatory test (***$p < 0.001$). **b** Representative immunoblot image of RT1 AW2 comparing VN, VI, GI and GN groups. A target band for RT1 AW2 at the expected apparent molecular weight (37 kDa) was observed. The total protein Coomassie R-350 staining of the PVDF membrane was used as the loading control. Densitometry analysis was performed to quantify the levels of RT1 AW2 in all four groups. Statistics was performed using Graph pad Prism 6 software. The *graph* is representing the results of two-way ANOVA and Tukey post hoc confirmatory test (***$p < 0.001$). Values are expressed as mean ± SD

Verification of individual proteins by immunoblotting

The proteins SEPT5_RAT, VDAC1_RAT, SODM_RAT and PRDX5_RAT were selected to be quantified for verification using immunoblotting and all the four proteins were in agreement with the previous 2DE quantification. The levels of all the four above-mentioned proteins were increased significantly in VI group when compared to VN group. However, GL2011 increased the protein levels in GI group significantly higher than in VI group indicating a drug effect. This effect of the drug was further seen in GN rats, where the levels of these proteins increased significantly when compared to VN rats (Fig. 7a–d).

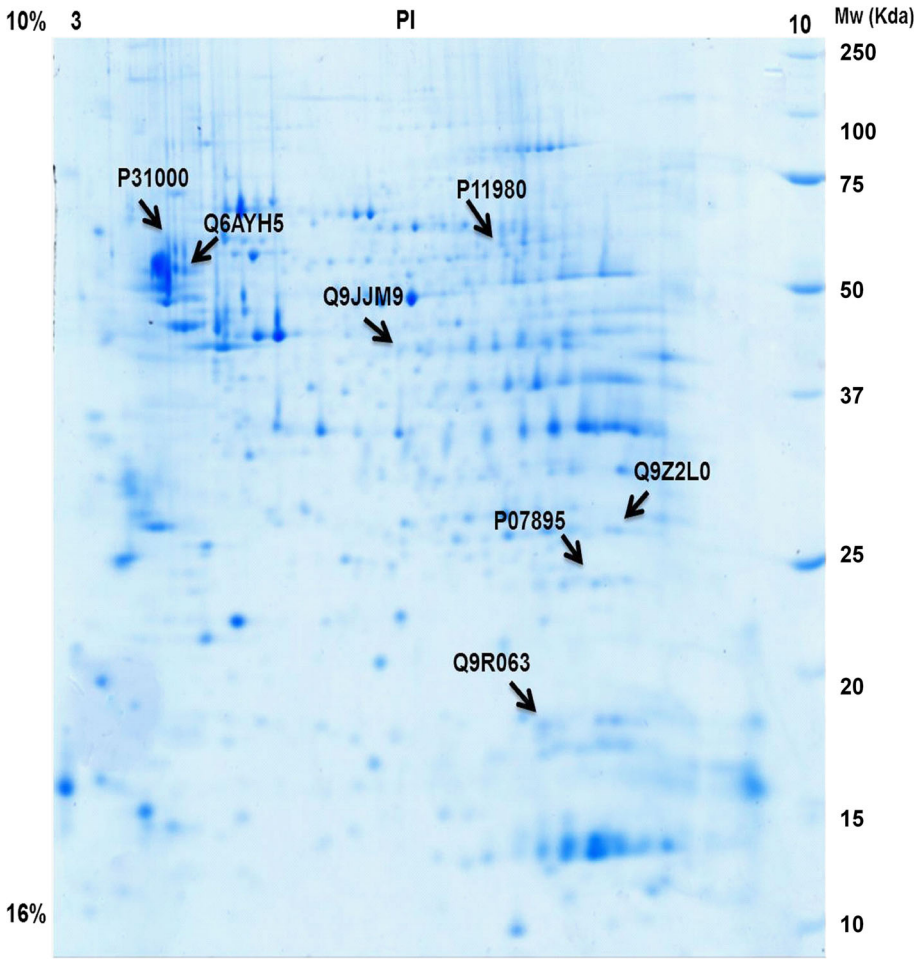

Fig. 6 Representative 2D electrophoresis image showing the spots with significantly different spot intensities among VN, VI, GN and GI groups. The protein spots which showed significantly different spot intensities among the four groups indicated by their given UniprotKB accession number (***$p < 0.001$, two-way ANOVA post hoc Tukey test)

Table 2 Mass spectrometrical identification of protein spots showing significantly different spot intensities between VN and VI groups

Spot number	UniProtKB accession number	Protein symbol/name	Nominal mass (M_r)	Score	Sequence coverage (%)	Enzyme	Species
1620	Q6AYH5	DCTN2_RAT/dynactin subunit 2	44,121	347	43	Trypsin	*Rattus norvegicus*
1708	P31000	VIME_RAT/vimentin	53,700	494	51	Trypsin	*Rattus norvegicus*
5512	Q9JJM9, Q8R2F7, Q9JJM8	SEPT5_RAT/septin 5	42,825	290	27	Trypsin	*Rattus norvegicus*
6105	Q9R063, Q68G22	PRDX5_RAT/peroxiredoxin 5	22,165	354	37	Trypsin	*Rattus norvegicus*
7210	P07895	SODM_RAT/superoxide dismutase [Mn], mitochondrial	24,659	420	45	Trypsin	*Rattus norvegicus*

Proteins significantly different between VI and VN, their corresponding spot numbers, UniprotKB accession numbers, nominal mass, score, sequence coverage and enzyme used for digestion for mass spectrometrical identification

Brain receptors

All levels of major brain receptor-containing complexes, as determined by blue-native gels and subsequent immunoblotting were comparable between groups without any significant difference except the D2-containing receptor complexes that were represented by two bands at approximately 720 kDa. The immunoblotting pattern of the D2-receptor-containing complexes is provided in Fig. 8. D2-containing receptor complex levels significantly increased in VI group when compared with VN group. GL2011 significantly decreased D2-receptor-containing complex levels in GI group when compared to VI group.

Discussion

The major outcome of the study is the result that a naturally occurring aminothiol, GL2011, is radioprotective against

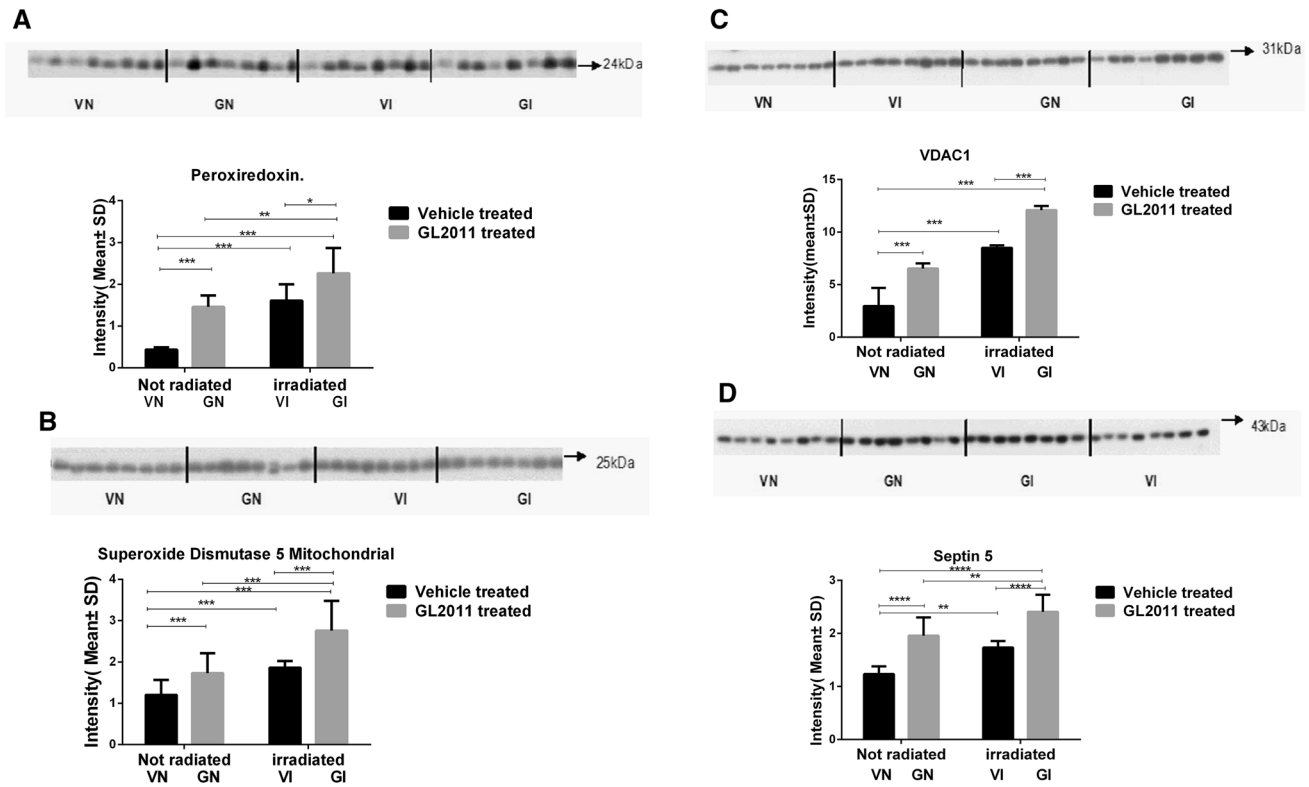

Fig. 7 Verification of 2D results by immunoblotting. **a** Representative immunoblot image comparing the levels of peroxiredoxin-5 in VN, VI, GI and GN groups. A target band for peroxiredoxin-5 at the expected apparent molecular weight (24 kDa) was observed. **b** Representative immunoblot image comparing the levels of superoxide dismutase-5 Mn in VN, VI, GI and GN groups. A target band for superoxide dismutase-5 Mn at the expected apparent molecular weight (25 kDa) was observed. **c** Representative immunoblot image of voltage-dependent anion-selective channel protein 1 comparing the levels of the protein in VN, VI, GI and GN groups. A target band for VDAC at the expected apparent molecular weight (31 kDa) was observed. **d** Representative immunoblot image of Septin-5 comparing the levels of the protein in VN, VI, GI and GN groups. A target band for Septin-5 at the expected apparent molecular weight (43 kDa) was observed. In all the experiments, the total protein Coomassie R-350 staining of the PVDF membrane was used as the loading control. The *graphs* represent the densitometry analysis performed to quantify the levels of the proteins using immunoblotting in all four groups. Statistics was performed using Graph pad Prism 6 software (two-way ANOVA and Tukey post hoc confirmatory test—$***p < 0.001$). Values are expressed as mean ± SD

whole-body irradiation at high doses of gamma irradiation. The drug GL2011, conferred commendable protection against a lethal dose of gamma irradiation when given in three identical doses at three time points to the rats included in the study. The survival percentage of GI rats was 93, as compared to the 30 % survival in VI rats.

The intestinal epithelium is sensitive to radiation injury (Riehl et al. 2012) and an excellent standard to study the radiation injury and the protective effects of a radioprotector like GL2011. As observed from jejunal crypt assay, the radiation had a potent effect on the villi and crypts as seen by the significantly reduced number of villi and crypt counts in VI group compared to VN, GN and GI group. The administration of GL2011 had no effect on the villi population in the GN group, indicating no severe effects of GL2011 on the intestinal epithelia. Also it was noted that the number of total, small- and medium-length villi as well as crypts of GI group was comparable to VN group, demonstrating a radioprotective effect of GL2011 for the GI tract.

The neuroprotective behavioural effects were demonstrated using the open field as well as the elevated plus maze. The administration of GL2011 to rats prior to and after irradiation significantly reversed the effect of radiation on resting time, average speed, path length, percentage of large movements and frequency of spontaneous changes in the open field. In elevated plus maze study, GL2011 reversed the effect of radiation on path length in the open arm and time spent in the open arm as compared to VI rats.

Searching for RNAs that may be involved in radiation damage and/or protection revealed that only two nucleic acids were potentially involved. Subsequently these two, Aadat and RT1 AW2, were confirmed at the protein level. Aadat, an enzyme of intermediary metabolism is involved in the metabolism of lysine that catalyses the reversible transamination reaction between L-2-aminoadipate and

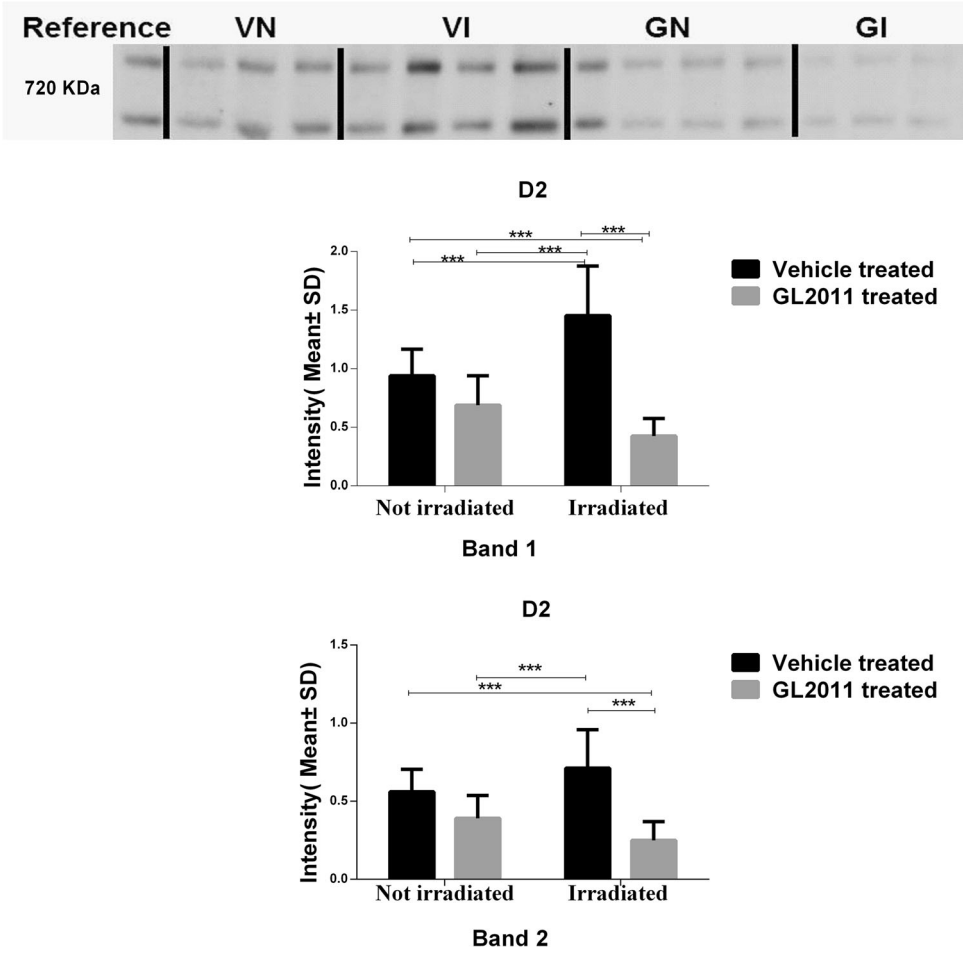

Fig. 8 Immunoblot of D2 receptor complex comparing the levels in VN, VI, GN and GI groups. Representative immunoblot image of D2 receptor-containing complexes comparing the levels in VN, VI, GN and GI groups. Two target bands for the D2 receptor complex at the expected apparent molecular weight (approx. 720 KDa) were observed. The total protein Coomassie R-350 staining of the PVDF membrane was used as the loading control. Densitometry analysis was performed to quantify the level of D2 receptor complex in all four groups. Statistics was performed using Graph pad Prism 6 software. The graph is representing the results of two-way ANOVA and Tukey post hoc confirmatory test (***$p < 0.001$). Values are expressed as mean ± SD

2-oxoglutarate to produce 2-oxoadipate and L-glutamate (Buchli et al. 1995) which in turn may be responsible for the reported glutamate-evoked excitotoxicity in the irradiated brain (Gliyazova et al. 2013). GL2011 reversed the increase of hypothalamic Aadat levels induced by irradiation. Immune cells are shown to be vulnerable to radiation. In our study RT1AW2, an RNA, belonging to the MHC I class family, with an immunoglobulin-like domain (entry name, HA11_RAT; accession number, P15978) showed increased expression in VI rats compared to VN rats, which was reversed by GL2011 in GI rats.

Septin 5 has been reported at the protein level (Diao et al. 2007), but no specific function has been assigned to this protein although involvement in cell cycle/cell division has been suggested (Kremer et al. 2007). Radiation increased septin 5 levels in the VI rats compared to the VN rats significantly which may present a possible mechanism to cope with radiation-induced cell damage by increasing the level of septin 5. Interestingly, the levels were increased more so in GN and GI rats compared to VN and VI groups, indicating the effect of GL2011 on septin 5 levels. Radiation also increased levels of VDAC1 in VI rats. The change of this porin may reflect altered metabolic fluxes following radiation or simply play a role in apoptosis (Craigen and Graham 2008). Accordingly, the levels of VDAC 1 were significantly increased in GN and GI rats as compared to VN and VI rats.

Reactive oxygen species play a key role in cell death following ionizing radiation (Morales et al. 1998). All cells contain a certain level of endogenous free radical scavengers, the expression of which can be induced under stressful conditions as radiation exposure. Several radioprotective compounds like amifostine can induce the expression of endogenous scavengers, and it is one of the most potent inducers of MnSOD (Murley et al. 2007). Superoxide dismutase has been shown to be involved in the radiation response and its effect on radiation protection has been reported (Hardmeier et al. 1997). Herein, two antioxidant enzymes, SODM_RAT and PRDX5_RAT showed increased levels in VI rats compared to VN rats which can be deciphered as the animal's innate mechanism to protect against radiation-induced oxidative stress. Levels of these proteins increased significantly in GI rats as compared to all other three groups, indicating the effect of GL2011 on

these proteins. GL2011 increased the protein levels in the absence of irradiation in GN rats strongly suggesting a drug effect raising the levels of antioxidant enzymes. This activity may be considered as a possible mechanism for the effective radioprotection observed although the aminothiol may act in vivo also as a prooxidant eliciting the increased antioxidant response. It is known that the peroxiredoxins are proteins which play an important role in the antioxidant defence and hydrogen peroxide-mediated signalling (Wood et al. 2003). However, so far no specific information is available on the possible role of PRDX5 in the mechanisms of radioprotection or radiation damage and this probable role is herewith proposed. Even in non-irradiated rats GL2011 is increasing brain levels of all the above-mentioned antioxidant enzymes.

Although there is no reported direct link between dopamine, its receptors and radiation, dopamine is involved in inducing apoptosis by an oxidation-mediated signalling pathway (Luo et al. 1999). The levels of a D2 receptor complex increased in VI rats as compared to VN rats, representing neuronal damage and subsequently one may conclude that the reversal of D2 levels in GI rats reflects the neuroprotective effect of GL2011.

Taken together, we have observed a significant radioprotective effect by a non-toxic naturally occurring aminothiol, GL2011 in terms of survival, intestinal crypt cell protection, behaviour and studied probable pathways and cascades potentially involved in ionizing radiation-induced damage and protection.

Conflict of interest The authors have declared that no conflict of interest exists.

References

Astapova I, Lee LJ, Morales C et al (2008) The nuclear corepressor, NCoR, regulates thyroid hormone action in vivo. Proc Natl Acad Sci USA 105:19544–19549. doi:10.1073/pnas.0804604105

Bae N, Lödl M, Pollak A, Lubec G (2012) Mass spectrometrical analysis of bilin-binding protein from the wing of *Hebomoia glaucippe* (Linnaeus, 1758) (Lepidoptera: Pieridae). Electrophoresis 33:1787–1794. doi:10.1002/elps.201100569

Belkacémi Y, Rat P, Piel G et al (2001) Lens epithelial cell protection by aminothiol WR-1065 and anetholedithiolethione from ionizing radiation. Int J Cancer 96(Suppl):15–26. doi:10.1002/ijc.10346

Bhattacharya R, Rao PV, Pant SC et al (2001) Protective effects of amifostine and its analogues on sulfur mustard toxicity in vitro and in vivo. Toxicol Appl Pharmacol 176:24–33. doi:10.1006/taap.2001.9252

Buchli R, Alberati-Giani D, Malherbe P et al (1995) Cloning and functional expression of a soluble form of kynurenine/α-aminoadipate aminotransferase from rat kidney. J Biol Chem 270:29330–29335. doi:10.1074/jbc.270.49.29330

Capizzi R (1996) Amifostine: the preclinical basis for broad-spectrum selective cytoprotection of normal tissues from cytotoxic therapies. Semin Oncol 23:2–17

Carnes BA, Grdina DJ (1992) In vivo protection by the aminothiol WR-2721 against neutron-induced carcinogenesis. Int J Radiat Biol 61:567–576

Chen P, Li X, Sun Y et al (2006) Proteomic analysis of rat hippocampal plasma membrane: characterization of potential neuronal-specific plasma membrane proteins. J Neurochem 98:1126–1140. doi:10.1111/j.1471-4159.2006.03934.x

Cotrim AP, Yoshikawa M, Sunshine AN et al (2012) Pharmacological protection from radiation ± cisplatin—induced oral mucositis. Int J Radiat Oncol Biol Phys 83:1284–1290. doi:10.1016/j.ijrobp.2011.09.026

Craigen WJ, Graham BH (2008) Genetic strategies for dissecting mammalian and Drosophila voltage-dependent anion channel functions. J Bioenerg Biomembr 40:207–212. doi:10.1007/s10863-008-9146-x

Dai M, Wang P, Boyd AD et al (2005) Evolving gene/transcript definitions significantly alter the interpretation of GeneChip data. Nucleic Acids Res 33:e175. doi:10.1093/nar/gni179

Devi PU, Bisht KS, Vinitha M (1998) A comparative study of radioprotection by *Ocimum* flavonoids and synthetic aminothiol protectors in the mouse. Br J Radiol 71:782–784. doi:10.1259/bjr.71.847.9771390

Diamond AM, Dale P, Murray JL, Grdina DJ (1996) The inhibition of radiation-induced mutagenesis by the combined effects of selenium and the aminothiol WR-1065. Mutat Res Mol Mech Mutagen 356:147–154. doi:10.1016/0027-5107(96)00016-4

Diao W-F, Höger H, Chen W-Q et al (2007) Hippocampal signaling protein levels are different in early and late metestrus in the rat. Biochim Biophys Acta BBA Proteins Proteomics 1774:1044–1051. doi:10.1016/j.bbapap.2007.05.002

Edwards CH, Gadsen EL, Edwards GA (1964) Methionine and homocysteine as protective agents against irradiation damage. Metabolism 13:373–380

Evans HH, Evans TE, Horng MF (2002) Antimutagenicity of WR-1065 in L5178Y cells exposed to accelerated (56)Fe ions. Radiat Res 158:110–114

Ghafari M, Patil SS, Höger H et al (2011) NMDA-complexes linked to spatial memory performance in the Barnes maze in CD1 mice. Behav Brain Res 221:142–148. doi:10.1016/j.bbr.2011.02.042

Gliyazova NS, Huh EY, Ibeanu GC (2013) A novel phenoxy thiophene sulphonamide molecule protects against glutamate evoked oxidative injury in a neuronal cell model. BMC Neurosci 14:93. doi:10.1186/1471-2202-14-93

Hardmeier R, Hoeger H, Fang-Kircher S et al (1997) Transcription and activity of antioxidant enzymes after ionizing irradiation in radiation-resistant and radiation-sensitive mice. Proc Natl Acad Sci USA 94:7572–7576

Irwin S (1968) Comprehensive observational assessment: Ia. A systematic, quantitative procedure for assessing the behavioral and physiologic state of the mouse. Psychopharmacologia 13:222–257

Kang SU, Fuchs K, Sieghart W, Lubec G (2008) Gel-based mass spectrometric analysis of recombinant GABAA receptor subunits representing strongly hydrophobic transmembrane proteins. J Proteome Res 7:3498–3506. doi:10.1021/pr800236u

Kremer BE, Adang LA, Macara IG (2007) Septins regulate actin organization and cell cycle arrest through SOCS7-mediated nuclear accumulation of NCK. Cell 130:837–850. doi:10.1016/j.cell.2007.06.053

Kumar KS, Srinivasan V, Toles R et al (2002a) Nutritional approaches to radioprotection: vitamin E. Mil Med 167:57–59

Kumar KS, Srinivasan V, Toles RE et al (2002b) High-dose antibiotic therapy is superior to a 3-drug combination of prostanoids and lipid A derivative in protecting irradiated canines. J Radiat Res (Tokyo) 43:361–370

Laayoun A, Coulombeau C, Constant JF et al (1994) Aminothiols linked to quinoline and acridine chromophores efficiently decrease 7,8-dihydro-8-oxo-2′-deoxyguanosine formation in gamma-irradiated DNA. Int J Radiat Biol 66:259–266

Littlefield LG, Hoffmann GR (1993) Modulation of the clastogenic activity of ionizing radiation and bleomycin by the aminothiol WR-1065. Environ Mol Mutagen 22:225–230

Logie LC, Harris MD, Tatsch RE, Van Hooser EN (1960) An analysis of the LD50(30) as related to radiation intensity. Radiat Res 12:349–356

Luo Y, Hattori A, Munoz J et al (1999) Intrastriatal dopamine injection induces apoptosis through oxidation-involved activation of transcription factors AP-1 and NF-κB in rats. Mol Pharmacol 56:254–264. doi:10.1124/mol.56.2.254

Mitrović O, Mićić M, Radenković G et al (2012) Endocrine cells in human fetal corpus of stomach: appearance, distribution, and density. J Gastroenterol 47:1212–1220. doi:10.1007/s00535-012-0597-9

Morales A, Miranda M, Sánchez-Reyes A et al (1998) Oxidative damage of mitochondrial and nuclear DNA induced by ionizing radiation in human hepatoblastoma cells. Int J Radiat Oncol 42:191–203. doi:10.1016/S0360-3016(98)00185-0

Murley JS, Kataoka Y, Baker KL et al (2007) Manganese superoxide dismutase (SOD2)-mediated delayed radioprotection induced by the free thiol form of amifostine and tumor necrosis factor alpha. Radiat Res 167:465–474. doi:10.1667/RR0758.1

Pellow S, Chopin P, File SE, Briley M (1985) Validation of open : closed arm entries in an elevated plus-maze as a measure of anxiety in the rat. J Neurosci Methods 14:149–167. doi:10.1016/0165-0270(85)90031-7

Perroy, Buchet (1953) Radiation protection with sulfhydryl-containing amino acids; experimental study. Sem Hôp Organe Fondé Par Assoc Enseign Méd Hôp Paris 29:1935–1939

Prouillac C, Vicendo P, Garrigues J-C et al (2009) Evaluation of new thiadiazoles and benzothiazoles as potential radioprotectors: free radical scavenging activity in vitro and theoretical studies (QSAR, DFT). Free Radic Biol Med 46:1139–1148. doi:10.1016/j.freeradbiomed.2009.01.016

Prut L, Belzung C (2003) The open field as a paradigm to measure the effects of drugs on anxiety-like behaviors: a review. Eur J Pharmacol 463:3–33. doi:10.1016/S0014-2999(03)01272-X

Rainer J, Sanchez-Cabo F, Stocker G et al (2006) CARMAweb: comprehensive R- and bioconductor-based web service for microarray data analysis. Nucleic Acids Res 34:W498–W503. doi:10.1093/nar/gkl038

Riehl TE, Foster L, Stenson WF (2012) Hyaluronic acid is radioprotective in the intestine through a TLR4 and COX-2-mediated mechanism. Am J Physiol Gastrointest Liver Physiol 302:G309–G316. doi:10.1152/ajpgi.00248.2011

Rogers DC, Peters J, Martin JE et al (2001) SHIRPA, a protocol for behavioral assessment: validation for longitudinal study of neurological dysfunction in mice. Neurosci Lett 306:89–92. doi:10.1016/S0304-3940(01)01885-7

Schuman VL, Clement JJ, Levitt SH, Song CW (1983) Skin radioprotection by 5-thio-D-glucose. Radiat Res 93:326–331

Smith PK, Krohn RI, Hermanson GT et al (1985) Measurement of protein using bicinchoninic acid. Anal Biochem 150:76–85. doi:10.1016/0003-2697(85)90442-7

Smyth GK (2005) Limma: linear models for microarray data. In: Gentleman R, Carey VJ, Huber W, Irizarry RA, Dudoit S (eds) Bioinformatics and computational biology solutions using R and Bioconductor. Statistics for biology and health. Springer, New York, pp 397–420

Vos O (1992) Role of endogenous thiols in protection. Adv Space Res Off J Comm Space Res COSPAR 12:201–207

Vuyyuri SB, Hamstra DA, Khanna D et al (2008) Evaluation of D-methionine as a novel oral radiation protector for prevention of mucositis. Clin Cancer Res 14:2161–2170. doi:10.1158/1078-0432.CCR-07-1954

Ware JH, Zhou Z, Romero-Weaver AL et al (2011) Effects of selenomethionine in irradiated human thyroid epithelial cells and tumorigenicity studies. Nutr Cancer 63:1114–1121. doi:10.1080/01635581.2011.605981

Wasserman TH, Brizel DM (2001) The role of amifostine as a radioprotector. Oncol Williston Park N 15:1349–1354 (discussion 1357–1360)

Welinder C, Ekblad L (2011) Coomassie staining as loading control in western blot analysis. J Proteome Res 10:1416–1419. doi:10.1021/pr1011476

Williams MV, Denekamp J (1983) Modification of the radiation response of the mouse kidney by misonidazole and WR-2721. Int J Radiat Oncol 9:1731–1736. doi:10.1016/0360-3016(83)90427-3

Wood ZA, Schröder E, Robin Harris J, Poole LB (2003) Structure, mechanism and regulation of peroxiredoxins. Trends Biochem Sci 28:32–40. doi:10.1016/S0968-0004(02)00003-8